

# PROMIST-5K: A COMPREHENSIVE DATASET FOR DIGITAL EMULATION OF CINEMATIC PRO-MIST FILTER EFFECTS

*Yingtie Lei<sup>1</sup>      Zimeng Li<sup>2</sup>      Chi-Man Pun<sup>1</sup>      Wangyu Wu<sup>3</sup>      Junke Yang<sup>4</sup>      Xuhang Chen<sup>1,5†</sup>*

<sup>1</sup> University of Macau, <sup>2</sup>Shenzhen Polytechnic University, <sup>3</sup>Xi'an Jiaotong-Liverpool University  
<sup>4</sup>University of Illinois Urbana-Champaign, <sup>5</sup> Huizhou University

## ABSTRACT

Pro-Mist filters are widely used in cinematography for their ability to create soft halation, lower contrast, and produce a distinctive, atmospheric style. These effects are difficult to reproduce digitally due to the complex behavior of light diffusion. We present ProMist-5K, a dataset designed to support cinematic style emulation. It is built using a physically inspired pipeline in a scene-referred linear space and includes 20,000 high-resolution image pairs across four configurations, covering two filter densities (1/2 and 1/8) and two focal lengths (20mm and 50mm). Unlike general style datasets, ProMist-5K focuses on realistic glow and highlight diffusion effects. Multiple blur layers and carefully tuned weighting are used to model the varying intensity and spread of optical diffusion. The dataset provides a consistent and controllable target domain that supports various image translation models and learning paradigms. Experiments show that the dataset works well across different training settings and helps capture both subtle and strong cinematic appearances. ProMist-5K offers a practical and physically grounded resource for film-inspired image transformation, bridging the gap between digital flexibility and traditional lens aesthetics. The dataset is available at <https://www.kaggle.com/datasets/yingtielei/promist5k>.

**Index Terms**— Computational photography, digital cinematography, optical filter emulation

## 1. INTRODUCTION

The advancement of digital sensors and computational imaging pipelines has reshaped photography and cinematography. Modern cameras provide sharpness, wide dynamic range, and precise tone control, yet digital images often appear overly sharp or “digital,” lacking the emotional depth that defines cinematic visuals. By contrast, cinematography is characterized by halation, smooth contrast transitions, and a nostalgic atmosphere [1]. These qualities are often achieved with optical filters. Neutral density filters regulate exposure [2], polarizers enhance saturation and control reflections [3], and color

correction filters balance temperature across lighting conditions [4].

Among these tools, Pro-Mist filters are especially valued for their ability to diffuse highlights and reduce contrast while preserving detail. Fine light-scattering particles in the glass scatter bright light into surrounding regions, lowering highlight intensity and lifting shadows. This creates a soft halo, smoother tonal transitions, and a more atmospheric appearance. Such effects enhance depth and emotional tone, aligning with the goals of professional cinematography. However, physical filters require multiple grades and diameters, interrupt on-set efficiency, and fix their effect irreversibly at capture. They also apply uniformly across the frame, offering no selective control.

Digital alternatives promise flexibility but face challenges. Many post-processing tools imitate glow or blur without modeling the underlying light scattering or operating in scene-referred space, often failing to reproduce the balance between halation, contrast attenuation, and detail preservation. Despite the importance of diffusion filters in filmmaking, faithful computational emulation remains underexplored. To address this gap, we introduce ProMist-5K, the first principled framework for digital emulation of Pro-Mist filters. By embedding physically inspired diffusion into a scene-referred pipeline, our method reproduces halation and tonal softness consistent with real filters. This contribution provides a controllable solution for post-production and establishes a foundation for future work in computational cinematography and optical effect emulation.

## 2. RELATED WORK

### 2.1. Realistic Cinematic Image Editing

Research on cinematic rendering has made progress in reproducing film-like qualities such as tonal response, grain, and depth of field, but the simulation of halation remains largely overlooked. Gong *et al.* [5] proposed Film-GAN to reproduce tonal response and grain, and Li *et al.* [1] built Film-Set, a dataset of 5,000 images with calibrated film styles for tone and color emulation. Other studies have extended this direction to perceptual attributes. Ameur *et al.* [6] introduced

† Corresponding Author



**Fig. 1.** Comparison of effects under different densities and focal lengths. At a fixed density, increasing the focal length from (a) to (b) intensifies highlight diffusion. At a fixed focal length, reducing the density from (a) to (c) weakens the softening effect. (d) shows that low density combined with longer focal length maintains a subtle yet visible cinematic atmosphere.

FilmGrainStyle740k for grain synthesis, Ignatov *et al.* [7] released the EBB! dataset for bokeh emulation, and Xian *et al.* [8] presented BETD with synthetic blur variations. These works have provided valuable resources for modeling film-like appearance, yet they focus mainly on tone, grain, and blur. None of them capture halation, which filmmakers regard as essential for conveying cinematic softness and atmosphere. Addressing this missing dimension is central to our work, as we aim to provide a principled framework for the emulation of Pro-Mist filters that reproduces this key optical effect.

## 2.2. Artistic Image Stylization

Artistic image stylization aims to transfer aesthetic qualities from artworks to photographs, focusing on creative transformation rather than real lens behavior. Early work by Gatys *et al.* [9] demonstrated that neural networks can separate content and style through feature statistics, which enabled style transfer from paintings to images. This line of research was extended by AdaIN [10] for real-time arbitrary style transfer and CycleGAN [11] for unpaired translation. More recently, diffusion-based methods such as InST [12] and StyleDiffusion [13] have improved consistency and preserved stylistic details. Several datasets support this task. WikiArt [14] is a widely used resource of artworks from diverse movements, and MS-COCO [15] provides content supervision. BAM! [16] adds labeled artworks from modern design, while StyleGallery [17] integrates WikiArt, JourneyDB [18], and LAION-Aesthetics [19] to cover a broad range of styles. Other benchmarks, such as BAID [20] and APDDv2 [21], include structured annotations to support evaluation. Although these datasets advance stylization research, they do not cap-

ture the physics-based optical properties of cinematography, which highlights the need for resources that reflect real lens effects.

## 3. PROMIST-5K DATASET

### 3.1. Dataset Description

We present ProMist-5K, a paired dataset designed for research in physically grounded cinematic image translation. It extends the Adobe-MIT FiveK dataset [22] and reproduces the distinctive visual behavior of Pro-Mist filters under realistic conditions. The dataset covers four filter settings that combine two diffusion strengths (1/2 and 1/8) with two focal lengths (20mm and 50mm). As summarized in Table 1, each configuration contains 4,500 training pairs and 500 testing pairs, resulting in a total of 20,000 high-resolution samples. Each pair consists of an emulated Pro-Mist image and its corresponding unfiltered original.

The interaction between density and focal length produces systematic differences in visual appearance, as shown in Fig. 1. At a fixed density of 1/2, increasing the focal length from 20mm to 50mm strengthens highlight diffusion and halation. At a constant focal length of 20mm, reducing the density from 1/2 to 1/8 weakens the softening while preserving more structural detail. Even with a low density of 1/8, a longer focal length of 50mm still introduces a subtle but noticeable cinematic glow.

To further illustrate the filter’s influence, Fig. 2 analyzes the 1/2@20mm setting in HSV color space. The diffusion of light reduces brightness peaks, compresses dynamic range, and smooths tonal transitions. It also lowers saturation, shifting distributions toward weaker color intensity. Hue remains relatively stable, but the reduction of peak values suggests a softening of dominant tones. These quantitative changes confirm how Pro-Mist filters balance highlight suppression, contrast reduction, and color desaturation, reinforcing their distinctive filmic aesthetic. This analysis highlights the value of ProMist-5K as a reliable benchmark for studying cinematic diffusion effects.

### 3.2. Dataset Construction

We construct the ProMist-5K dataset through an emulation pipeline designed to reproduce the optical behavior of physical Pro-Mist filters. As shown in Fig. 3, the pipeline operates

**Table 1.** Summary of the ProMist-5K Dataset

Configuration	Training	Testing	Visual Effect Description
1/8 @ 20mm	4,500	500	Subtle diffusion with high detail retention
1/8 @ 50mm	4,500	500	Mild halation with balanced contrast
1/2 @ 20mm	4,500	500	Strong bloom with softened contrast
1/2 @ 50mm	4,500	500	Heavy diffusion with dramatic cinematic glow
Total	18,000	2,000	Comprehensive range of cinematic effects

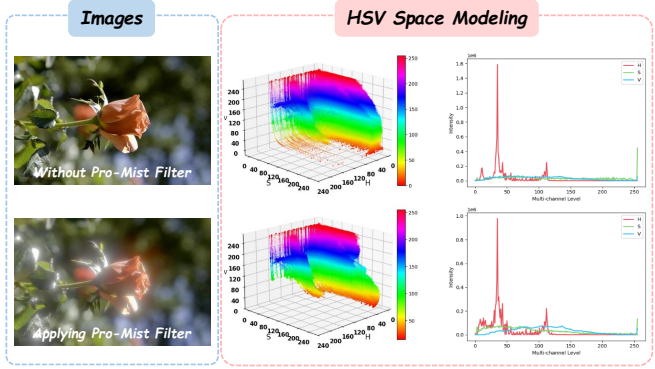


**Fig. 2.** Pro-Mist filter effect (1/2@20mm): Original vs. filtered image with their 3D HSV space models and 1D histograms. Altered HSV distributions illustrate highlight suppression, contrast reduction, and desaturation.

in a scene-referred linear color space, where pixel values are proportional to real-world light intensities. This setting enables accurate modeling of how bright regions scatter light into surrounding areas, producing the halation and glow typical of diffusion filters. Each image is first converted to the linear space by removing gamma encoding, which allows subsequent operations to simulate physical light behavior more faithfully.

To approximate diffusion, we apply six Gaussian blur layers with progressively larger kernels. These layers represent different scattering scales produced by particles inside a real filter. The perceived filter density is controlled by adjusting the blending weights of these blurred layers. In the 1/2 density setting, larger-radius layers dominate and produce stronger halos. In the 1/8 setting, smaller-radius layers are emphasized, leading to softer diffusion and better preservation of structure. Fig. 4 demonstrates how increasing the number of blur layers improves spatial richness and tonal smoothness, yielding a more natural result. The pipeline also accounts for

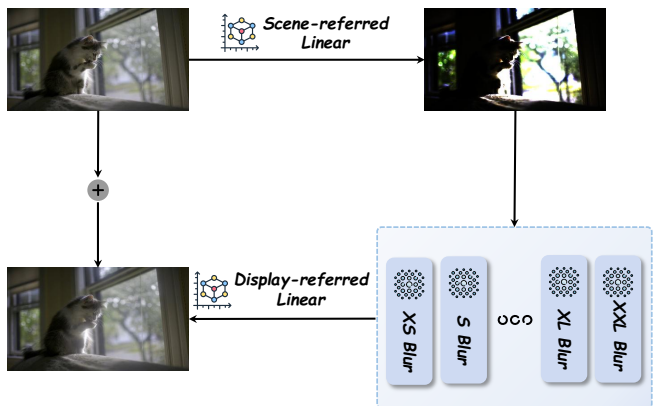


**Fig. 3.** Pro-Mist Filter Emulation Pipeline.

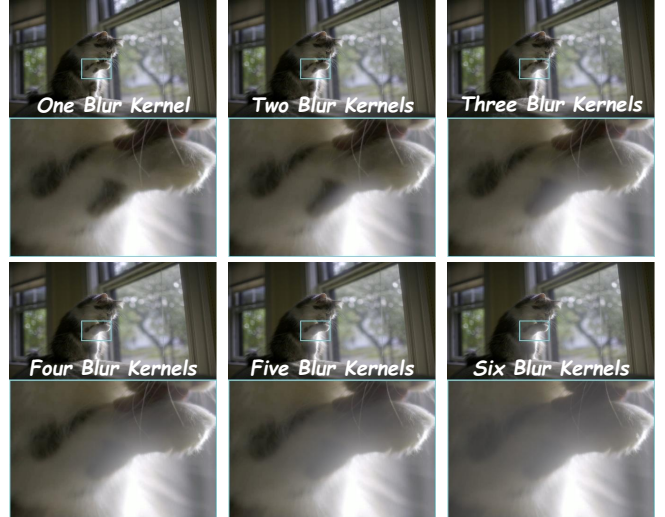


**Fig. 4.** Contribution of Multi-Scale Blur Layers to Pro-Mist Emulation. Increasing the number of blur layers improves the fidelity of halation rendering.

focal length. At the same density, images captured at longer focal lengths such as 50mm are simulated with larger blur radii than those at 20mm. This adjustment matches the more pronounced and spatially concentrated halation of telephoto lenses. After applying the appropriate blur weighting and kernel scaling, the blurred layers are combined with the original scene-referred image. The result is then tone-mapped to a display-referred format. Each stylized image is paired with its unfiltered counterpart, creating a supervised training pair. In total, the dataset contains 20,000 pairs evenly distributed across four configurations. These samples form a benchmark for tasks such as highlight diffusion, halation emulation, and broader cinematic enhancement.

## 4. BASELINE EVALUATION

### 4.1. Baselines and Experimental Setup

Image-to-image translation seeks to convert an image from one domain to another while preserving structure and semantics. In our case, the goal is to transform a clean digital image into a stylized version that reproduces the visual effects of a Pro-Mist filter. ProMist-5K is particularly suitable for this task because it provides high-resolution paired images that include both the unfiltered input and its emulated counterpart with halation and highlight diffusion. This design supports paired and unpaired translation approaches and creates a consistent domain grounded in physical principles, which helps models learn in a stable and generalizable way.

To assess the dataset, we evaluate several representative translation models: CycleGAN [11], Pix2Pix [23], DualGAN [24], UNIT [25], DRIT [26], and LPTN [27]. These

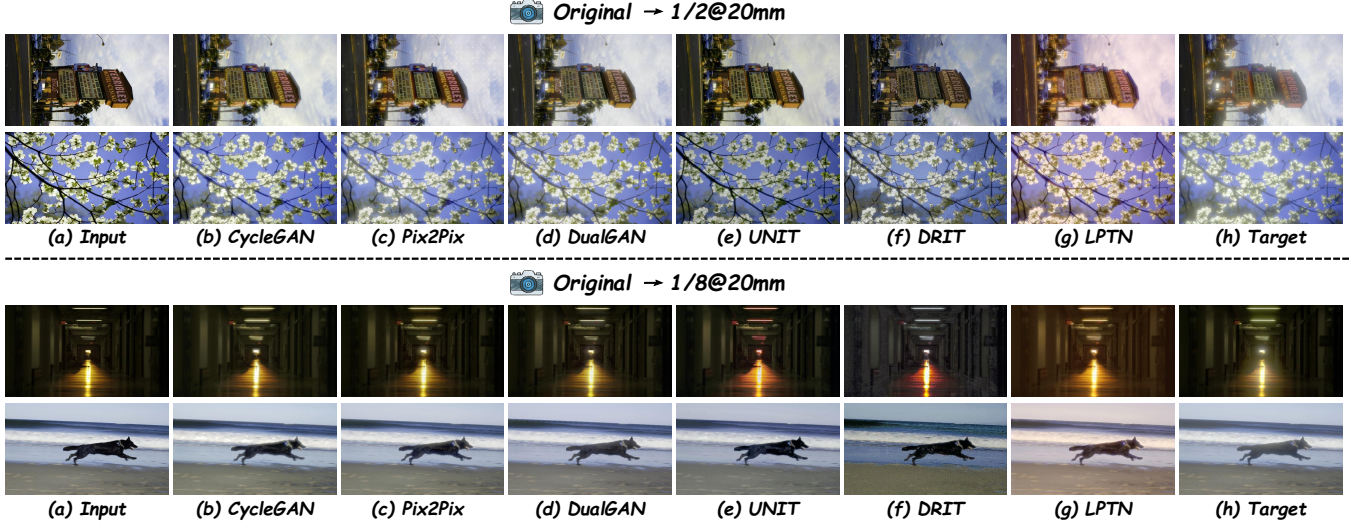


**Fig. 5.** Qualitative comparison of different translation models on two representative Pro-Mist emulation tasks (Original → 1/2@20mm and Original → 1/8@20mm).

**Table 2.** Quantitative evaluation results on two Pro-Mist emulation tasks (Original → 1/2@20mm and Original → 1/8@20mm) using PSNR, SSIM, LPIPS, and FID. The best score for each metric is shown in red, and the second-best is shown in blue.

Methods	Original → 1/2@20mm				Original → 1/8@20mm			
	PSNR↑	SSIM↑	LPIPS↓	FID↓	PSNR↑	SSIM↑	LPIPS↓	FID↓
CycleGAN [11]	24.6045	0.9114	0.0717	57.9102	28.7285	0.9478	0.0329	31.2321
Pix2Pix [23]	<b>26.3893</b>	<b>0.9154</b>	<b>0.0618</b>	<b>49.1602</b>	<b>30.1434</b>	<b>0.9592</b>	<b>0.0257</b>	<b>25.1520</b>
DualGAN [24]	<b>25.9989</b>	<b>0.9252</b>	<b>0.0664</b>	<b>54.6365</b>	<b>29.4912</b>	<b>0.9584</b>	<b>0.0310</b>	<b>30.5926</b>
UNIT [25]	20.6195	0.8648	0.1070	71.4165	24.0747	0.9256	0.0511	43.2495
DRIT [26]	18.4447	0.7752	0.1674	86.1399	19.4654	0.8094	0.1244	68.3024
LPTN [27]	21.3794	0.8870	0.1003	64.8371	21.6460	0.9112	0.0559	42.0154

baselines cover both paired and unpaired training and are widely used in image translation research. All experiments are run on an NVIDIA RTX A6000 GPU using the official implementations with default settings. Each model is trained for 200 epochs with a batch size of 8. We report results on two representative tasks: translating original images to the 1/2@20mm version and to the 1/8@20mm version. These two settings differ in the strength and spread of highlight diffusion, which allows us to test performance on both pronounced and subtle emulation cases.

## 4.2. Results and Analysis

Table 2 shows the overall performance of different models under two filter settings. Paired model like Pix2Pix perform more reliably, especially in capturing soft halation and preserving image structure. Unpaired models like CycleGAN and DualGAN also show reasonable results, which suggests that the dataset can be used in both supervised and unsupervised settings without major limitations. Fig. 5 provides visual examples that reflect these differences. For the

1/2@20mm task, models need to reproduce stronger glow and wider light spread, which is more difficult to model. Paired models produce smoother and more natural-looking transitions, while unpaired models may introduce blur artifacts or color inconsistencies around highlights. In the 1/8@20mm case, where the diffusion is more subtle, most models generate cleaner results with better detail preservation.

These results confirm that ProMist-5K supports a wide range of image translation tasks. It provides a consistent setting for evaluating both subtle and strong diffusion effects, and allows fair comparison across different model types.

## 5. CONCLUSION

This work introduces ProMist-5K, a dataset for emulating Pro-Mist filter effects that are widely used in cinematography to create softness and atmosphere. Unlike methods that apply generic artistic filters, our dataset follows physically consistent principles and reproduces optical characteristics such as halation, glow diffusion, and contrast reduction with control and accuracy. The scene-referred emulation pipeline models lens behavior under different densities and focal lengths, enabling fine-grained reproduction of subtle cues. Comprehensive evaluation demonstrates that ProMist-5K offers a strong foundation for analyzing and learning cinematic diffusion effects. It supports flexible experimentation with data-driven approaches and addresses a gap in existing resources by focusing on lens behaviors that are central to storytelling and emotional tone. We expect this dataset to facilitate future research in stylization, post-production, and computational cinematography, contributing to more expressive and controllable image creation.

## 6. ACKNOWLEDGMENT

This work was supported in part by the Science and Technology Development Fund, Macau SAR, under Grant 0193/2023/RIA3 and 0079/2025/AFJ, in part by the University of Macau under Grant MYRG-GRG2024-00065-FST-UMDF, and in part by the Guangdong Basic and Applied Basic Research Foundation (Grant No. 2024A1515140010).

## 7. REFERENCES

- [1] Zinuo Li, Xuhang Chen, et al., “A large-scale film style dataset for learning multi-frequency driven film enhancement,” in *IJCAI*, 2023, pp. 1160–1168.
- [2] Virgil-Florin Duma, Mirela Nicolov, et al., “Neutral density filters with risley prisms: analysis and design,” *Applied optics*, vol. 48, no. 14, pp. 2678–2685, 2009.
- [3] Lawrence B Wolff, Andreas G Andreou, et al., “Polarization camera sensors,” *Image and Vision Computing*, vol. 13, no. 6, pp. 497–510, 1995.
- [4] Michael J Vrheil, H Joel Trussell, et al., “Filter considerations in color correction,” *IEEE Transactions on image processing*, vol. 3, no. 2, pp. 147–161, 1994.
- [5] Haoyan Gong, Jionglong Su, et al., “Film-gan: towards realistic analog film photo generation,” *Neural Computing and Applications*, vol. 36, no. 8, pp. 4281–4291, 2024.
- [6] Zoubida Ameur, Claire-Hélène Demarty, et al., “Style-based film grain analysis and synthesis,” in *ACM MM*, 2023, pp. 229–238.
- [7] Andrey Ignatov, Jagruti Patel, et al., “Rendering natural camera bokeh effect with deep learning,” in *CVPR Workshops*, 2020, pp. 418–419.
- [8] Marcos V Conde, Manuel Kolmet, et al., “Lens-to-lens bokeh effect transformation. ntire 2023 challenge report,” in *CVPR*, 2023, pp. 1643–1659.
- [9] Leon A Gatys, Alexander S Ecker, et al., “Image style transfer using convolutional neural networks,” in *CVPR*, 2016, pp. 2414–2423.
- [10] Xun Huang, Serge Belongie, et al., “Arbitrary style transfer in real-time with adaptive instance normalization,” in *ICCV*, 2017, pp. 1501–1510.
- [11] Jun-Yan Zhu, Taesung Park, et al., “Unpaired image-to-image translation using cycle-consistent adversarial networks,” in *ICCV*, 2017, pp. 2223–2232.
- [12] Yuxin Zhang, Nisha Huang, et al., “Inversion-based style transfer with diffusion models,” in *CVPR*, 2023, pp. 10146–10156.
- [13] Zhizhong Wang, Lei Zhao, et al., “Stylediffusion: Controllable disentangled style transfer via diffusion models,” in *ICCV*, 2023, pp. 7677–7689.
- [14] Fred Phillips, Brandy Mackintosh, et al., “Wiki art gallery, inc.: A case for critical thinking,” *Issues in Accounting Education*, vol. 26, no. 3, pp. 593–608, 2011.
- [15] Tsung-Yi Lin, Michael Maire, et al., “Microsoft coco: Common objects in context,” in *ECCV*. Springer, 2014, pp. 740–755.
- [16] Michael J Wilber, Chen Fang, et al., “Bam! the behance artistic media dataset for recognition beyond photography,” in *ICCV*, 2017, pp. 1202–1211.
- [17] Junyao Gao, Yanchen Liu, et al., “Styleshot: A snapshot on any style,” *arXiv preprint arXiv:2407.01414*, 2024.
- [18] Keqiang Sun, Junting Pan, et al., “Journeydb: A benchmark for generative image understanding,” *NeurIPS*, vol. 36, pp. 49659–49678, 2023.
- [19] Christoph Schuhmann, Romain Beaumont, et al., “Laion-5b: An open large-scale dataset for training next generation image-text models,” *NeurIPS*, vol. 35, pp. 25278–25294, 2022.
- [20] Ran Yi, Haoyuan Tian, et al., “Towards artistic image aesthetics assessment: a large-scale dataset and a new method,” in *CVPR*, 2023, pp. 22388–22397.
- [21] Xin Jin, Qianqian Qiao, et al., “APDDv2: Aesthetics of paintings and drawings dataset with artist labeled scores and comments,” in *The Thirty-eight Conference on Neural Information Processing Systems Datasets and Benchmarks Track*, 2024.
- [22] Vladimir Bychkovsky, Sylvain Paris, et al., “Learning photographic global tonal adjustment with a database of input/output image pairs,” in *ICCV*, 2011, pp. 97–104.
- [23] Phillip Isola, Jun-Yan Zhu, et al., “Image-to-image translation with conditional adversarial networks,” in *CVPR*, 2017, pp. 1125–1134.
- [24] Zili Yi, Hao Zhang, et al., “Dualgan: Unsupervised dual learning for image-to-image translation,” in *ICCV*, 2017, pp. 2849–2857.
- [25] Ming-Yu Liu, Thomas Breuel, et al., “Unsupervised image-to-image translation networks,” *NeurIPS*, vol. 30, 2017.
- [26] Hsin-Ying Lee, Hung-Yu Tseng, et al., “Diverse image-to-image translation via disentangled representations,” in *ECCV*, 2018, pp. 35–51.

[27] Jie Liang, Hui Zeng, et al., “High-resolution photorealistic image translation in real-time: A laplacian pyramid translation network,” in *CVPR*, 2021, pp. 9392–9400.